CrystEngComm

Accepted Manuscript

ROYAL SOCIETY OF CHEMISTRY

www.rsc.org/crystengcomm

Cite this: DOI: 10.1039/c0xx00000x

www.rsc.org/xxxxxx

ARTICLE TYPE

Structures and properties of coordination polymers involving asymmetric biphenyl-3,2′,5′-tricarboxylate

Jie Zhao,[a] Li-Qiong Xie,[a] Ying-Ming Ma,[a] Ai-Ju Zhou,[a] Wen Dong,[a] Jing Wang*[a], Yan-Cong Chen[b] and Ming-Liang Tong[b]

Received (in XXX, XXX) Xth XXXXXXXXX 20XX, Accepted Xth XXXXXXXXX 20XX
DOI: 10.1039/b000000x

An asymmetric polycarboxylate ligand, biphenyl-3,2′,5′-tricarboxylic acid (H_3bptc) with rotatable coordination vertex, was employed to react with metal ions under hydrothermal conditions. Four new coordination polymers $\{[Mn_3(bptc)_2(4,4'\text{-bpy})_3(H_2O)_2]\}_n$ (**1**), $\{Ni(Hbptc)(4,4'\text{-bpy})_{1.5}(H_2O)_2]\cdot H_2O\}_n$ (**2**), $\{[Cd_2(Hbptc)_2(phen)_4]\cdot 3H_2O\}_n$ (**3**) and $\{[Cu_2(Hbptc)_2(2,2'\text{-bpy})_2(H_2O)_2]\cdot 2H_2O\}_n$ (**4**) were successfully synthesized and characterized. Single crystal X-ray analysis reveals that compound **1** has a 3D coordination network with linear Mn(II)$_3$-based subunits, while **2** is a 1D ladder chain-based structure further interconnected by hydrogen bonds to 3D supramolecular network. Compounds **3** and **4** have a hydrogen bonds and π···π interactions supported supramolecular network consisting of different dimmers $[Cd_2(Hbptc)_2(phen)_4]$ and $[Cu_2(Hbptc)_2(2,2'\text{-bpy})_2]$. The conformations' stability and coordination modes of H_3bptc ligand has been discussed, the magnetic and fluorescent properties have been investigated.

Introduction

Much research into coordination polymers based on metal centres and multifunctional bridging ligands has been attractive in the field of materials science due to their fascinating structures and new topologies, as well as their tremendous potential applications as functional materials including catalysis, gas storage, fluorescent sensing, electronic and magnetic devices.[1] More and more efforts have mainly focused on the construction and preparation of versatile coordination polymers, as well as the structure–property relationships. The structure information stored in the organic ligands along with the coordination geometry of the metal ions should be taken into account. Therefore, the judicious choice and design of organic moieties is very important for constructing novel structures and searching new bridging ligands has a great interest and challenge.[2] Many construction features of ligands could affect the structural assembly process of these materials, such as the size and shape, the flexibility and the functional groups within the ligands. [3]

Polycarboxylate ligands have been proven to be good candidates for constructing novel structures because they can be regarded not only as hydrogen-bonding acceptors but also as the donors, depending on the number of deprotonated carboxylic groups. Of the aromatic carboxylates, the rigid 1,4-benzenedicarboxylate,[4] 1,3,5-benzenetricarboxylate,[5] 1,2,4,5-benzenetetracarboxylate,[6] 1,2,3,4,5-benzenepentacarboxylate[7] and 1,2,3,4,5,6-benzenehexacarboxylate[8] are studied extensively to construct numerous coordination polymers. Compared to rigid aromatic ligands, the semi-rigid biphenyl ligands possess more flexibility because of the free rotation of the C-C bond between the phenyl rings and therefore may build coordination polymers with more diverse structures. More recently, versatile coordination polymers assembled from biphenyl carboxylate ligands, such as biphenyldicarboxylate,[9] biphenyl-3,4′,5-tricarboxylate,[10] and biphenyl-3,5,3′,5′/3,4,3′,4′/2,4,2′,4′-tetracarboxylate [11] compounds have been reported. Most of these polycarboxylate ligands possess highly symmetric geometry which is suitable to result symmetric networks. In contrast, coordination polymers based on asymmetric polycarboxylate ligands are far less prevalent, probably due to the asymmetric geometry making it difficult to predict and control the final coordination networks.[12]

To the best of our knowledge, coordination polymers based on biphenyl-3,2′,5′-tricarboxylic acid (H_3bptc) have been rarely documented.[13] H_3bptc as one type of bridging biphenyl polycarboxylate ligand has rotatable coordination vertex and asymmetric geometry with three carboxylate groups. Learning from our previous study on conformational flexible cyclohexane-polycarboxylate coordination polymers,[14] the H_3bptc with rotatable coordination vertex and asymmetric geometry may be a good candidate for constructing versatile coordination networks with functional properties. With the introduction of an auxiliary ligand, such as 4,4′-bipyridine (4,4′-bpy), 1,10-phenanthroline (phen) and 2,2′-bipyridine (2,2′-bpy) into the reaction system, four new coordination polymers have been obtained. Herein, we report the syntheses and structural characterizations of four new coordination polymers, $\{[Mn_3(bptc)_2(4,4'\text{-bpy})_3(H_2O)_2]\}_n$ (**1**), $\{Ni(Hbptc)(4,4'\text{-bpy})_{1.5}(H_2O)_2]\cdot H_2O\}_n$ (**2**), $\{[Cd_2(Hbptc)_2(phen)_4]\cdot 3H_2O\}_n$ (**3**), $\{[Cu_2(Hbptc)_2(2,2'\text{-bpy})_2(H_2O)_2]\cdot 2H_2O\}_n$ (**4**), which exhibit a systematic variation of architectures from a 0D dimmer to a 3D framework constructed

from deprotonated H_3bptc and auxiliary ligands. The conformations' stability and coordination modes of H_3bptc ligand have been discussed. In addition, the magnetic and fluorescent properties have been investigated.

Experimental section

Materials and methods

The reagents and solvents employed were commercially available and used as received without further purification. The C, H, and N microanalyses for the four compounds were performed on fresh sample, with Elementar Vario-EL CHN elemental analyzer. FT-IR spectra were recorded from KBr pellets in the range of 4000-400 cm^{-1} on a Bio-Rad FTS-7 spectrometer. X-ray powder diffraction (XRPD) intensities for the four compounds were measured at 293 K on a Bruker D8 X-ray diffratometer (Cu-Kα, λ = 1.54056 Å). The crushed poly-crystalline powder samples were prepared by crushing the crystals and scanned from 5-60^o with a step of 0.1^o/s, and calculated patterns were generated with PowderCell. Thermogravimetric (TG) analyses were carried out on NETZSCH TG209F3 thermogravimetric analyzer. Variable-temperature magnetic susceptibility measurements were performed on a SQUID magnetometer MPMS (Quantum Design) at 1.0 kOe for **1, 2**, **4,** and the diamagnetic correction was applied from Pascal's constants. The emission/excitation spectra for **1-4** were measured on an F-4500 Fluorescence Spectrophotometer.

Synthesis of $\{[Mn_3(bptc)_2(4,4'\text{-bpy})_3(H_2O)_2]\}_n$ (1)

A mixture of H_3bptc (0.053g, 0.20 mmol) and 4,4′-bpy (0.156 g, 1.00 mmol) in H_2O (5.0 mL) were added to an aqueous solution (12.0 mL) of $Mn(OAc)_2{\cdot}4H_2O$ (0.123 g, 0.50 mmol) and stirred. The resultant solution was heated in a stainless steel reactor with Teflon liner at 120 ^{o}C for 120h. After a period of approximately 12h's cooling to room temperature, colorless block crystals of **1** (yield *ca.* 78% based on Mn) were obtained, isolated by filtration and washed with water. IR (KBr, cm^{-1}): 3626w, 3072w, 2367w, 1582s, 1385s, 1224w, 1073w, 819m, 784m, 714w, 645m, 518w. Elemental analysis Calcd for $C_{30}H_{21}N_3O_7Mn_{1.50}$: C, 58.31; H, 3.43; N, 6.80. Found: C, 58.99; H, 3.10; N, 6.95.

Synthesis of $\{[Ni(Hbptc)(4,4'\text{-bpy})_{1.5}(H_2O)_2]{\cdot}H_2O\}_n$ (2)

A mixture of H_3bptc (0.053g, 0.20 mmol) and 4,4′-bpy (0.156 g, 1.00 mmol) in H_2O (5.0 mL) were added to an aqueous solution (12.0 mL) of $Ni(NO_3)_2{\cdot}6H_2O$ (0.114 g, 0.50 mmol) and stirred. The resultant solution was heated in a stainless steel reactor with Teflon liner at 120 ^{o}C for 168h. After a period of approximately 12h's cooling to room temperature, green block crystals of **2** (yield *ca.* 80% based on Ni) were obtained, isolated by filtration and washed with water. IR (KBr, cm^{-1}): 3615m, 3442m, 3118m, 2587w, 2367w, 1709s, 1628s, 1570vs, 1408vs, 1373vs, 1224s, 1073m, 923w, 796s, 680m, 623m, 507w. Elemental analysis Calcd for $C_{30}H_{26}N_3O_9Ni$: C, 57.08; H, 4.15; N, 6.66. Found: C, 58.21; H, 4.10; N, 6.85.

Synthesis of $\{[Cd_2(Hbptc)_2(phen)_4]{\cdot}3H_2O\}_n$ (3)

A mixture of H_3bptc (0.053g, 0.20 mmol) and phen (0.180 g, 1.00 mmol) in H_2O (5.0 mL) were added to an aqueous solution (12.0 mL) of $Cd(NO_3)_2{\cdot}4H_2O$ (0.122 g, 0.50 mmol) and stirred. The resultant solution was heated in a stainless steel reactor with Teflon liner at 120 ^{o}C for 120h. After a period of approximately 12h's cooling to room temperature, colorless block crystals of **3** (yield *ca.* 70% based on Cd) were obtained, isolated by filtration and washed with water. IR (KBr, cm^{-1}): 3049w, 2367w, 1720s, 1547vs, 1407vs, 1373s, 1224s, 1097m, 853s, 726s, 645w, 506w. Elemental analysis Calcd for $C_{78}H_{54}N_8O_{15}Cd_2$ (%): C, 59.74; H, 3.47; N, 7.15. Found: C, 62.12; H, 3.25; N, 7.45.

Synthesis of $\{[Cu_2(Hbptc)_2(2,2'\text{-bpy})_2(H_2O)_2]{\cdot}2H_2O\}_n$ (4)

A mixture of H_3bptc (0.027g, 0.10 mmol) and 2,2′-bpy (0.078 g, 0.50 mmol) in H_2O (5.0 mL) were added to an aqueous solution (12.0 mL) of $Cu(NO_3)_2{\cdot}3H_2O$ (0.089 g, 0.50 mmol) and stirred. The resultant solution was heated in a stainless steel reactor with Teflon liner at 120 ^{o}C for 72h. After a period of approximately 12h's cooling to room temperature, blue needle-like crystals of **4** (yield *ca.* 75% based on Cu) were obtained, isolated by filtration and washed with water. IR (KBr, cm^{-1}): 3049w, 2367w, 1709m, 1604vs, 1582vs, 1397s, 1362vs, 1246m, 1038w, 761m, 715w. Elemental analysis Calcd for $C_{25}H_{20}N_2O_8Cu$: C, 55.61; H, 3.73; N, 5.19. Found: C, 55.44; H, 3.68; N, 5.25.

Computational details

All of the structures were optimized using the Becke three-parameter Lee–Yang–Parr (B3-LYP) exchange-correlation functional method[15] with the 6-31G(d,p) basis sets[16] (Fig. S1). The stable configuration of the structures was confirmed by the vibrational frequency analysis, in which no imaginary frequency was found for the configuration at the energy minima. The sum of the electronic and thermal free energies was used to compare stability (Tab. S1). All of the calculations were performed with the Gaussian 09 computational package.[17]

Single-crystal structure determination

The data collection and structural analysis of crystals **1–4** were performed on a SMART (Bruker, 2002) diffractometer equipped with Mo-Kα radiation (λ= 0.71073 Å) at 296(2) K. Absorption corrections were applied by using multi-scan program SADABS. The structure was solved with direct methods and refined with a full-matrix least-squares technique with the SHELXTL program package.[18] Anisotropic thermal parameters were applied to all non-hydrogen atoms. The organic hydrogen atoms were generated geometrically (C-H 0.96 Å), the water hydrogen atoms were located from difference maps and refined with isotropic temperature factors. Crystal data as well as details of data collection and refinements are summarized in Table 1. Selected bond lengths and bond angles are listed in Table S2. Crystallographic data for the structures reported in this paper have been deposited in the Cambridge Crystallographic Data Center with CCDC reference number of 996435-996438 for compounds **1**-**4**.

Table 1 Crystallographic data and refinement parameters for compounds **1**-**4**.

Compound	**1**	**2**	**3**	**4**
Empirical formula	$C_{60}H_{42}N_6O_{14}Mn_3$	$C_{30}H_{26}N_3O_9Ni$	$C_{78}H_{54}N_8O_{15}Cd_2$	$C_{50}H_{40}N_4O_{16}Cu_2$

Fw	1235.82	631.25	1568.09	1079.94
Crystal system	monoclinic	triclinic	monoclinic	triclinic
Space group	$P2_1/n$	P-1	$C2/c$	P-1
a (Å)	9.3553(2)	9.5251(6)	25.6565(6)	7.4693(5)
b(Å)	24.7637(4)	9.8837(6)	12.4636(3)	9.9564(7)
c (Å)	11.6174(2)	16.3942(11)	21.2198(6)	15.8573(11)
α (°)	90.00	72.834(4)	90.00	81.091(5)
β (°)	113.4110(10)	87.431(4)	105.910(2)	88.095(4)
γ (°)	90.00	71.093(4)	90.00	69.091(4)
V (Å^3)	2469.86(8)	1392.88(15)	6525.6(3)	1088.01(13)
Z	2	2	4	1
D_c (g cm^{-3})	2.042	1.505	1.596	1.647
μ (mm^{-1})	3.871	0.759	0.732	1.062
F(000)	1457	654	3176	554
Reflections collected	39660	22494	24648	17461
R_{int}	0.0465	0.0385	0.0702	0.0286
Gof	1.047	1.062	0.985	1.034
Final R indices [$I > 2\sigma(I)$]	$R_1{}^a = 0.0344$	$R_1{}^a = 0.0388$	$R_1{}^a = 0.0440$	$R_1{}^a = 0.0319$
	$wR_2{}^b = 0.0814$	$wR_2{}^b = 0.0936$	$wR_2{}^b = 0.0867$	$wR_2{}^b = 0.0835$
R indices (all data)	$R_1{}^a = 0.0513$	$R_1{}^a = 0.0566$	$R_1{}^a = 0.0785$	$R_1{}^a = 0.0395$
	$wR_2{}^b = 0.0881$	$wR_2{}^b = 0.1062$	$wR_2{}^b = 0.0964$	$wR_2{}^b = 0.0876$
CCDC number	996438	996437	996435	996436

$^aR_1 = \sum||F_o|-|F_c||/\sum|F_o|$, $^b wR_2 = [\sum w(F_o^2-F_c^2)^2/\sum w(F_o^2)^2]^{1/2}$

Results and discussion

Theoretical calculations on free H_3bptc and coordination modes of the deprotonated bptc^{3-}/ Hbptc^{2-}

The biphenyl-3,2′,5′-tricarboxylic acid (H_3bptc) has rotatable coordination vertex and asymmetric geometry with three carboxylate groups (Scheme 1). The main conformational degrees of the free H_3bptc involve the rotation of the C-C bond between the two phenyl rings. Theoretical calculation shows that the thermodynamically most stable conformation is the one with dihedral angle 53.5º between the two phenyl rings in gas phase. The energy of the molecule is increasing with the dihedral angle changed and reaches to the maximum when the phenyl rings are close to be coplanar (Fig. S1).

According to our previous studies on coordination polymers on flexible ligands, the size and versatile coordination environments of the metal ions may play an important role in controlling the conformation of the flexible ligands.[11] In the present H_3bptc system, four metal ions were used, Mn(II), Ni(II), Cd(II) and Cu(II), resulting in different conformations and coordination modes of the ligand (Fig. 1). The dihedral angles between two phenyl rings in compounds **1**-**4** are 47.3º, 56.6º, 42.2º and 35.4º, respectively (Tab. S2). The fully deprotonated bptc^{3-} ligand in compound **1** adopts μ_5:η^2,η^2,η^1 bridging mode, while the partly deprotonated Hbptc^{2-} ligands adopt μ_2:η^1,η^1 in compounds **2** and **4**, μ_2:η^2 in compound **3**. It should be noted that the different conformation and coordination modes of the ligands not only relate to the metal ions, but also to the auxiliary ligands.

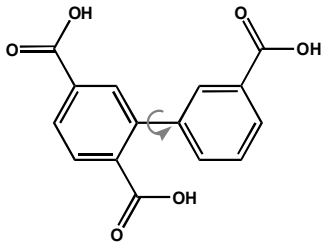

Scheme 1 biphenyl-3,2′,5′-tricarboxylic acid (H_3bptc)

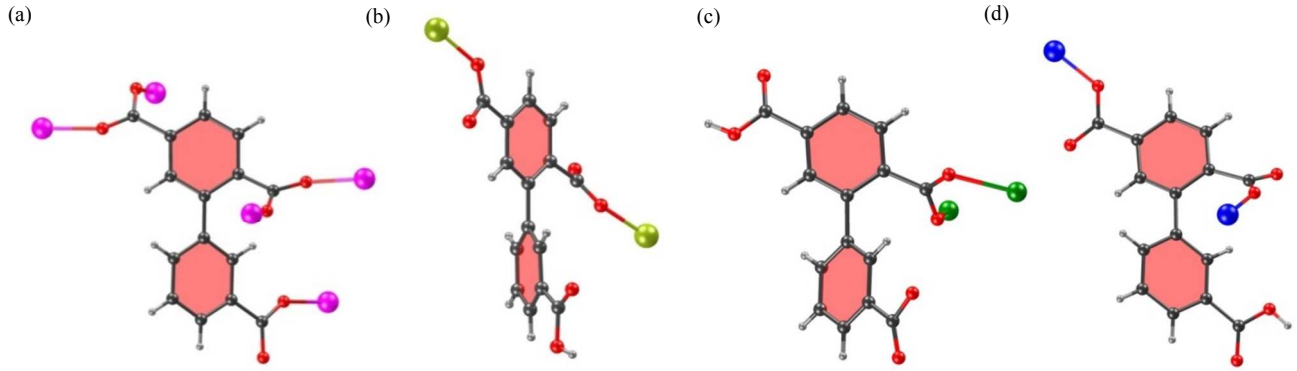

Fig. 1 The coordination modes of bptc^{3-}/ Hbptc^{2-} in compounds **1** (a)**, 2** (b)**, 3** (c) **and 4** (d).

Structure description

{[$Mn_3(bptc)_2(4,4'\text{-}bpy)_3(H_2O)_2$]}$_n$ (1)

X-ray crystallographic study of **1** reveals an infinite 3D coordination network based on linear $Mn(II)_3$-subunit that crystallizes in monoclinic space group $P2_1/n$. The asymmetric unit contains two crystallographically Mn(II) atoms (one of which lies on an inversion centre), one deprotonated $bptc^{3-}$, two 4,4′-bpy ligands (one of which lies on an inversion centre), one coordinated water molecule (Fig. 2a). Mn1 adopts a slightly distorted octahedral geometry, coordinating to three carboxylate oxygen atoms (O1, O4A, O6B) from three $bptc^{3-}$, one water oxygen atom (O1W), and two nitrogen atoms (N1, N2C) from two different 4,4′-bpy. Mn2 on an inversion centre also adopts an octahedral geometry, coordinating to four carboxylate oxygen atoms (O2, O5B, O2D, O5E) from four $bptc^{3-}$ and two nitrogen atoms (N3, N3D) from two symmetric 4,4′-bpy ligands. The bond lengths of Mn-O(carboxylate) fall in the range 2.1383(15)-2.2055(13) Å, the axial Mn-O(water) is 2.2767(17) Å, and Mn-N in the range 2.2691(15)-2.2740(15) Å (Table S2). The $bptc^{3-}$ ligand with a dihedral angle 47.3° of two phenyl rings is fully depronated. The three depronated carboxylate groups have different coordination modes including monodentate and bridging μ_2-η^1:η^1, to link five Mn(II) atoms (Fig. 1). The bridging carboxylate groups from four distinctive ligands bind three Mn(II) atoms into a linear $Mn(II)_3$-building unit (Fig. 2b). Each trinuclear unit connects six $bptc^{3-}$ ligands (Fig. 2b), while each two $bptc^{3-}$ ligands connecting four trinuclear units (Fig. 2c). The trinuclear subunits are linked by the μ_5-bridging $bptc^{3-}$ ligands to form a 3D coordination network (Fig. 2e). Meanwhile, there are two kinds of bridging 4,4′-bpy, one of which lies across a 2-fold axis and the other is asymmetric with a dihedral angle 29.2° between the two pyridyl rings. A 3D condensed framework is thus generated by the connection of the $bptc^{3-}$ ligands and 4,4′-bpy with no lattice water molecules (Fig. 2e). There are intramolecular hydrogen bonds between the coordinated water and uncoordinated carboxylate group (O1W···O3a = 2.698(2) Å, O1W-H1WA···O3a = 170(4)°, a: x, y, z+1).

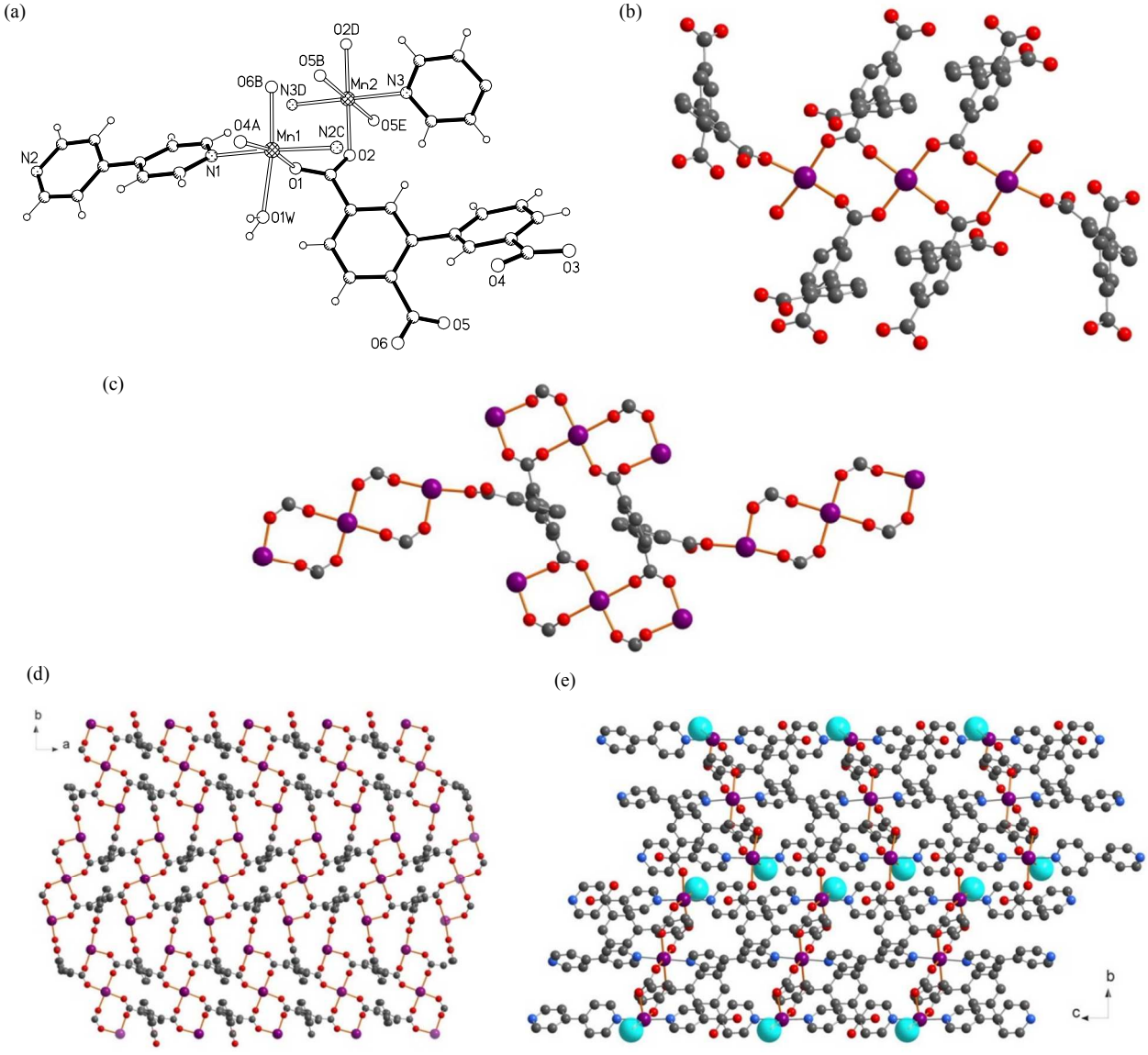

Fig. 2 (a) View of the coordination environments of Mn(II) atoms (A: x-1/2,-y+1/2,z+1/2; B: x-1,y,z; C: x,y,z-1; D: -x,-y,-z; E: -x+1,-y,-z)**;** (b) the linear $Mn(II)_3$-building unit**;** (c) the coordination of each two $bptc^{3-}$ ligands surrounded by four linear $Mn(II)_3$-subunits**;** (d) the 3D coordination network bridged by $bptc^{3-}$ ligands along the *c*-axis (4,4′-bpy are omitted for clarity)**;** (e) the 3D coordination framework bridged by $bptc^{3-}$ ligands and 4,4′-bpy (the coordinated water molecules in the framework are highlighted in sky blue spheres) in **1**.

$\{[Ni(Hbptc)(4,4'\text{-bpy})_{1.5}(H_2O)_2]\cdot H_2O\}_n$ (2)

X-ray crystallographic study of **2** reveals a supramolecular network based on 1D coordinated ladder chains that crystallizes in triclinic space group *P*-1. The asymmetric unit contains one crystallographically Ni(II) atom, one partly deprotoned $Hbptc^{2-}$, two 4,4′-bpy ligands (one of which lies on an inversion centre), two coordinated and one lattice water molecules (Fig. 3a). Ni1 adopts a slightly distorted octahedral geometry, coordinating to two carboxylate oxygen atoms (O2, O3A) from two $Hbptc^{2-}$, two water oxygen atom (O1W, O2W), and two nitrogen atoms (N1, N3) from two different 4,4′-bpy. The bond lengths of Ni-N are 2.0596(18) and 2.0943(19) Å, Ni-O(water) 2.0908(17) and 2.0921(18) Å, and Ni-O(carboxylate) 2.0597(15) and 2.0634(15) Å (Table S2). The $Hbptc^{2-}$ ligand with a dihedral angle 56.6º of two phenyl rings is partly depronated through the 2′,5′-carboxylate groups (Fig. 1). The partly deprotoned $Hbptc^{2-}$ adopts μ_2-bridging coordinated mode through two deprotoned carboxylate group in the same phenyl ring, connecting the Ni(II) atoms to form a 1D Ni-Hbptc chain (Fig. 3b). There are two kinds of 4,4′-bpy ligands adopting monodentate and μ_2-bridging coordination modes, respectively. The μ_2-bridging 4,4′-bpy lying on an inversion centre connects two Ni-Hbptc chains to form a 1D ladder chain, and the monodentate 4,4′-bpy with a dihedral angle 20.6º between two pyridyl rings are arrayed along both sides of the chain (Fig. 3b). The ladder chains are zipped together through their uncoordinated carboxylate groups and mondodentate 4,4′-bpy by hydrogen bonds (Fig. 3c). Thus, a 3D supramolecuar network with 1D channels occupied by water molecules is generated (Fig. 3d) and further strengthened by rich hydrogen bonds between carboxylate groups, 4,4′-bpy and water molecules. (O···O = 2.664(3)-3.137(3) Å, O-H···O= 151-172º) (Table S3).

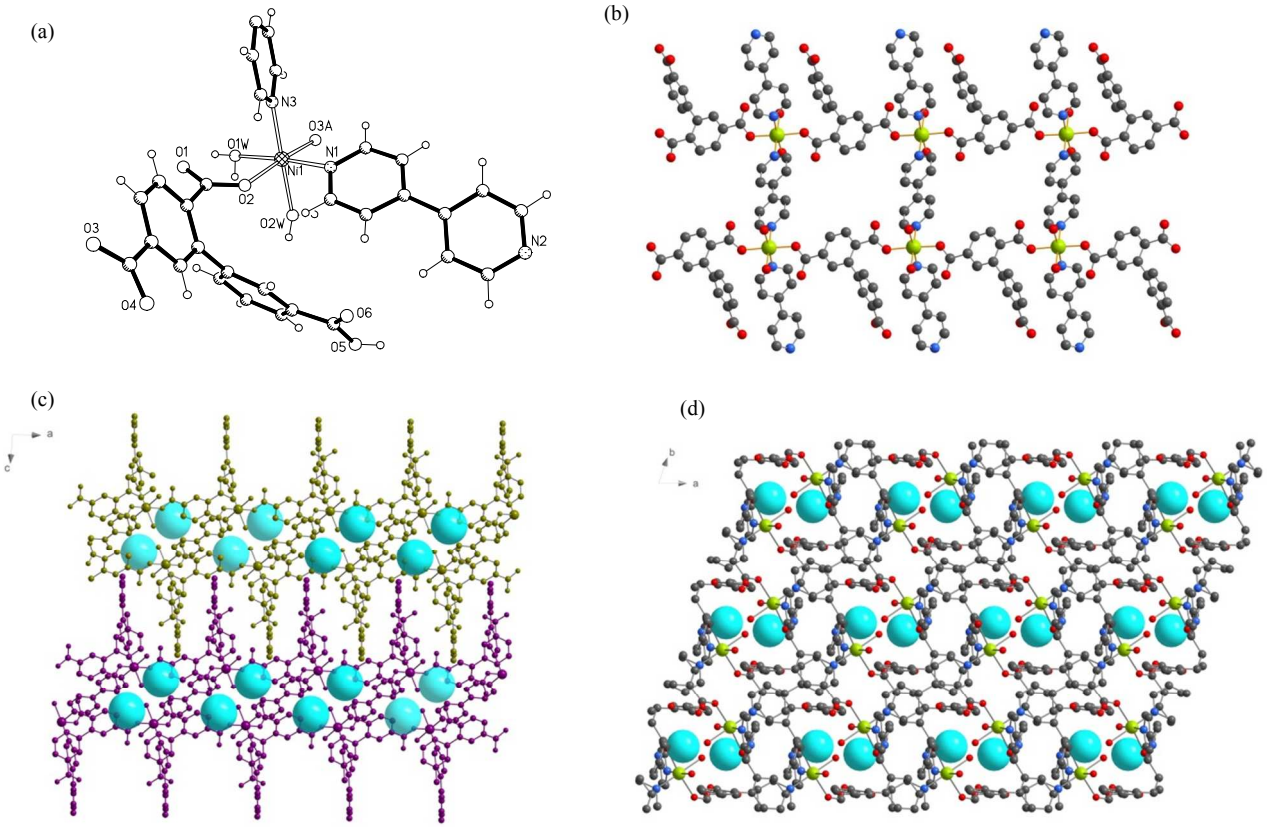

Fig. 3 (a) View of the coordination environment of Ni(II) atom (A: x+1,y-1,z)**;** (b) the 1D ladder chain bridged by $Hbptc^{2-}$ ligands 4,4′-bpy**;** (c) the adjacent ladder chains zipped together through their uncoordinated carboxylate groups and mondodentate 4,4′-bpy by hydrogen bonds viewed along the *b*-axis (the lattice water molecules are highlighted in sky blue spheres)**;** (d) the 3D supramolecular framework with 1D channels viewed along the *c*-axis (the lattice water molecules in the channels are highlighted in sky blue spheres) in **2**.

$\{[Cd_2(Hbptc)_2(phen)_4]\cdot 3H_2O\}_n$ (3)

X-ray crystallographic study reveals that **3** crystallizes in the monoclinic system *C*2/*c* space group. The asymmetric unit contains one crystallographically Cd(II) atoms, one partly deprotoned $Hbptc^{2-}$, two phen ligands and three disordered lattice

water molecules. Cd1 lies on a general position and has six-coordinated distorted octahedral geometry, coordinating to two carboxylate oxygen (O1, O2A) from two $Hbptc^{2-}$ and four nitrogen atoms (N1, N2, N3, N4) from two phen (Fig. 4a). The bond lengths of Cd-O are 2.246(2) and 2.270(3) Å) and Cd-N fall between 2.298(3) and 2.432(3) Å (Table S2). The $Hbptc^{2-}$ ligand with a dihedral angle 42.2º of two phenyl rings is partly depronated through the 3,2′-carboxylate groups (Fig. 1c). The partly deprotoned $Hbptc^{2-}$ connects two Cd(II) atoms in μ_2-bridging coordinated mode through its deprotoned 2′-carboxylate group. Two $Hbptc^{2-}$ ligands and four phen connects two Cd(II) atoms to form a dimmer building block $[Cd_2(Hbptc)_2(phen)_4]$, which lies on an inversion centre (Fig. 4b). The dimmers connect to each other to form a 1D chain via hydrogen-bonds between the deprotoned and undeprotoned carboxylate groups. Furthermore, adjacent chains are held together via π···π interactions between phen into a 3D supramolecular network (Fig. 4c). The shortest distance between the two parallel phen planes is 3.7Å, which is within the common range for π···π interactions between the two phenyl rings. There are hydrogen-bonds between the partly deprotoned carboxylate groups with half-occupancy hydrogen atom (O4···O4*a* = 2.430(5) Å, O4-H···O4*a* = 115º, *a*: -x, y, -z+3/2). The three disordered lattice water molecules are removed by using the SQUEEZE procedure and can be easily lost above room temperature because of the hydrophobic effects of molecules.

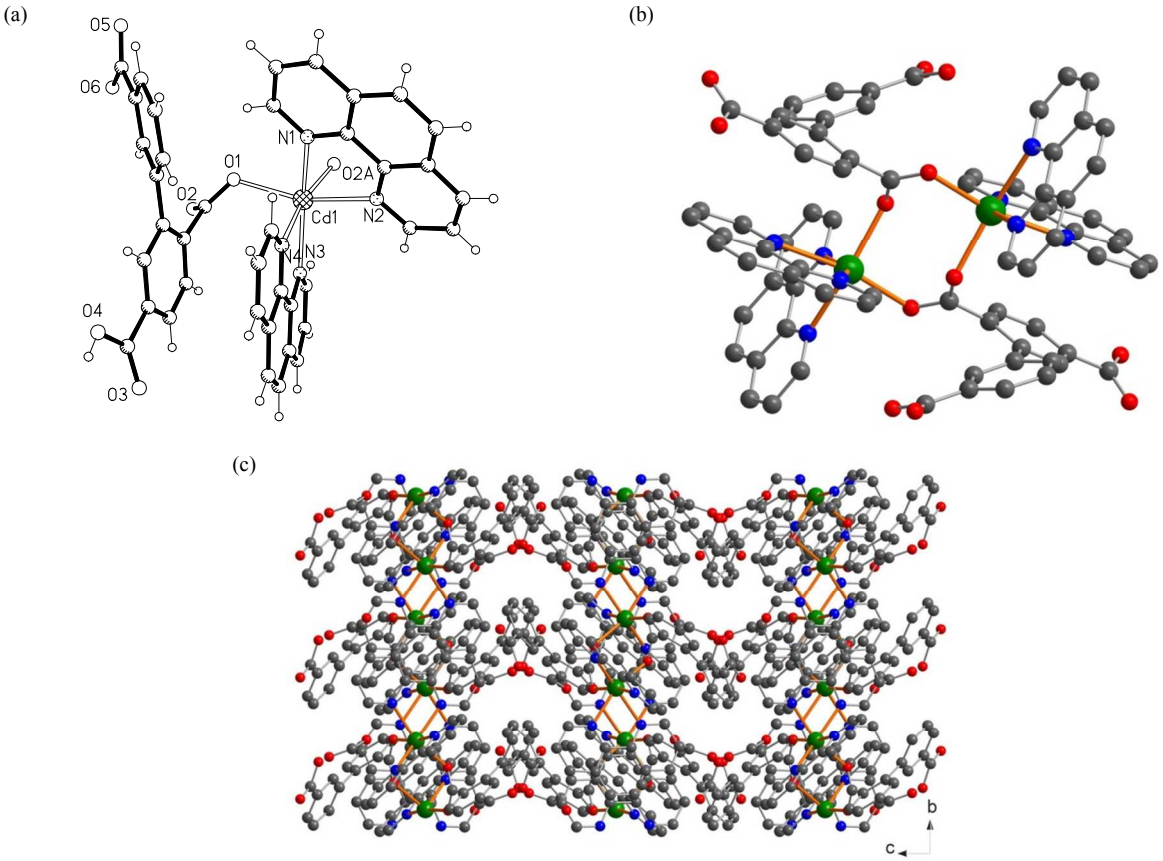

Fig. 4 (a) View of the coordination environment of Cd(II) atom (A: -x+1/2,-y+3/2,-z+1)**;** (b) the dimmer building block $[Cd_2(Hbptc)_2(phen)_4]$**;** (c) the 3D packed supramolecular network via π···π interactions viewed along the *a*-axis in **3**.

$\{[Cu_2(Hbptc)_2(2,2'\text{-bpy})_2(H_2O)_2]\cdot 2H_2O\}_n$ (4)

X-ray crystallographic study of **4** reveals a supramolecular network based on $[Cu_2(Hbptc)_2(2,2'\text{-bpy})_2]$ dimmers that crystallizes in triclinic space group *P*-1. The asymmetric unit contains one crystallographically Cu(II) atoms, one partly deprotoned $Hbptc^{2-}$, one 2,2′-bpy ligands, one coordinated and one lattice water molecules. Cu1 adopts a slightly distorted tetragonal pyramidal geometry, coordinating to two carboxylate oxygen atoms (O2, O4A) from two $Hbptc^{2-}$, one water oxygen atom (O1W), and two nitrogen atoms (N1, N2) from one 2,2′-bpy (Fig. 5a). The bond lengths of Cu-N are 1.9929(16) and 2.0089(16) Å. The axial Cu-O(water) bond lengths (2.2187(15) Å) is much longer than the equatorial Cu-O(carboxylate) (1.9115(13) and 1.9904(13) Å) (Table S2). The $Hbptc^{2-}$ ligand with a dihedral angle 35.4º of two phenyl rings is partly depronated through the 2′,5′-carboxylate groups (Fig. 1d). The partly deprotoned $Hbptc^{2-}$ connects two Cu(II) atoms in μ_2-bridging coordinated mode through two deprotoned carboxylate group. Two $Hbptc^{2-}$ ligands and two 2,2′-bpy connects two Cu(II) atoms to form a dimmer building block, which lies on an inversion centre (Fig. 4b). Due to the different bridging modes of the $Hbptc^{2-}$ ligand in **3** and **4**, the Cu···Cu distance 9.4 Å in the $[Cu_2(Hbptc)_2(2,2'\text{-bpy})_2]$ dimmer is much longer than Cd···Cd distance 4.6 Å in the $[Cd_2(Hbptc)_2(phen)_4]$ dimmer. The adjacent dimmers are held

together to form a 1D chains via π···π interactions with distance 3.3 Å between the phenyl ring of $Hbptc^{2-}$ ligand and pyridyl ring of 2,2′-bpy (Fig. 5c). Furthermore, rich hydrogen bonds between the water molecules and the carboxylate groups connects the chains to a 3D supramolecular network (O···O = 2.638(3)-3.023(2) Å, O-H···O= 157(4)-175(2)°) (Table S3).

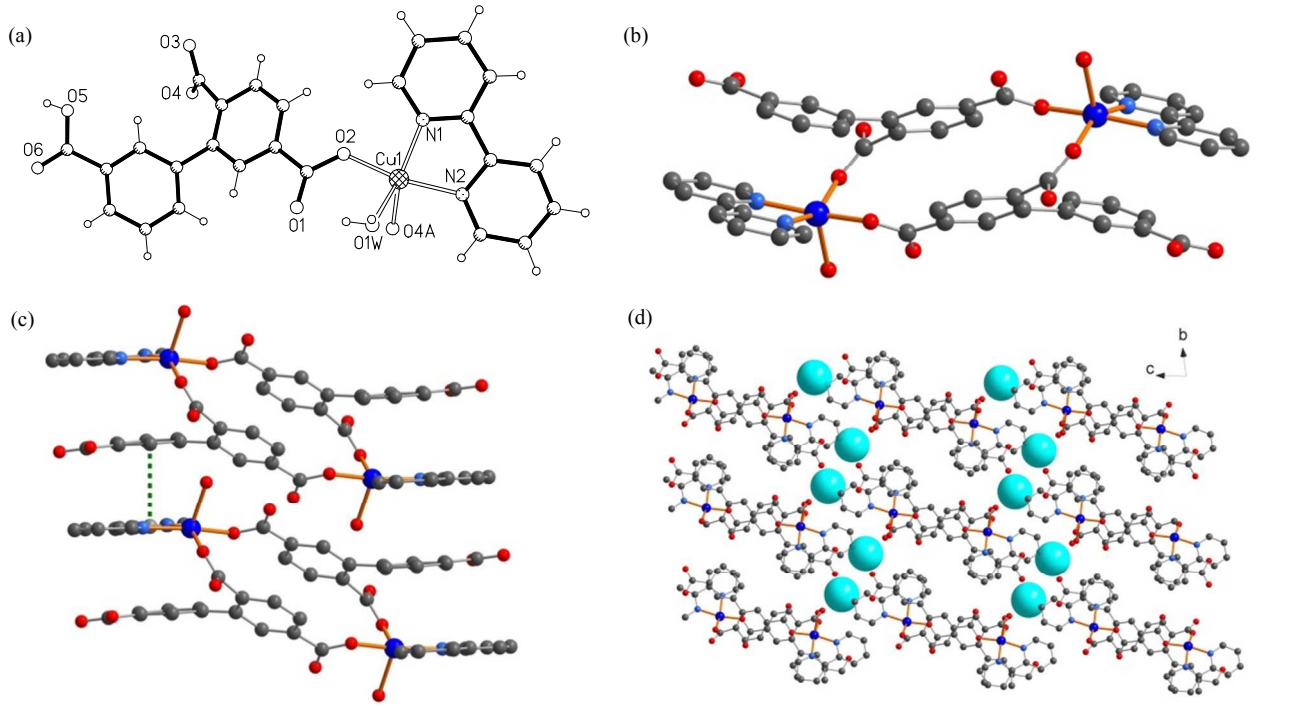

Fig. 5 (a) View of the coordination environment of Cu(II) atom (A: -x+2,-y+1,-z+1)**;** (b) the dimmer building block $[Cu_2(Hbptc)_2(2,2'\text{-bpy})_2]$**;** (c) the π···π interactions between the phenyl and pyridyl from adjacent dimmers (the hydrogen atoms are omitted for clarity)**;** (d) the stacking supramolecular network with lattice water molecules viewed along the *a*-axis (the lattice water molecules in the channels are highlighted in sky blue spheres) in **4**.

Thermal stability analysis

The measurement of the XRPD patterns were carried out at room temperature to conform the phase purity of compounds **1**–**4**. As shown in Figure S2, the peak positions of the simulated and experimental XRPD patters are in agreement with each other, demonstrating the good phase purity of the four compounds.

In order to examine the thermal stabilities of the four compounds, the thermal gravimetric (TG) analyses were carried out in dry nitrogen atmosphere from 30 to 650 °C (Fig. S3). For compound **1**, the TGA curve shows that the first weight loss of 3.0% at the beginning of 80 °C to 140 °C corresponds to the loss of the coordinated water molecule (calcd 2.9%) of one unit cell, and then the network is decomposed from 300 °C. The remaining weight of 17.2% indicates that the final product is MnO (calcd 17.2%). Compound **2** loses the lattice and coordinated water molecules (calcd 8.7% and expt 8.8%) from the beginning to 150 °C and then the supramolecular network is decomposed quickly resulting in the residue NiO (calcd 11.8% and expt 10.0%). For compound **3**, two disordered water molecules have been lost at room temperature because of the hydrophobic effects of molecules. The third water molecule (calcd 1.1% and expt 1.1%) was lost from the beginning to 80 °C and the network collapses among the temperature range 280-620 °C, which indicates it is thermally stable over a wide range of temperature. The observed weight losses including three steps between 280 °C and 620 °C before the final formation of CdO can be assigned to the elimination of the phen and $Hbpt^{2-}$ ligands. For compound **4**, the TGA curve shows that the first weight loss of 3.2% from the beginning to 90 °C corresponds to the loss of the lattice water molecule (calcd 3.3%) of one unit cell, and then the coordinated water molecule is lost up to 150 °C. The network is stable from 150 °C to 265 °C and then collapses quickly before the final formation of metal oxide.

Magnetic property

Variable temperature magnetic susceptibility was measured for compound **1** in a 1 kOe dc field. At 300 K, the experimental $\chi_M T$ values is 13.0 $cm^3 \cdot mol^{-1} \cdot K$, which is consistent with the expected value (13.125 $cm^3\ mol^{-1}\ K$) for three Mn(II) ions ($S = {}^5/_2$, $g = 2$) (Fig. 6a). Upon cooling, the $\chi_M T$ value keeps decreasing to 3.89 $cm^3\ mol^{-1}\ K$ at 1.8 K, and fitting the experimental data to the Curie-Weiss law in the temperature range of 10-300 K leads to an antiferromagnetic Weiss constant θ = -7.1 K (Fig. 6b). The dominating antiferromagnetic interaction in **1** can also be implied by the unsaturated magnetization values of 11.6 Nβ at 2 K and 70 kOe (compared with the expected 15 Nβ) (Fig. 6c). Moreover, due to the symmetrical linear Mn(II) trimmer sub-structure of **1**, the magnetic susceptibility can also be satisfactorily fitted to the exchange model by the spin Hamiltonian: [19]

$$\hat{H} = -2\sum_{i=1}^{n}\sum_{j>i}^{n} J_{ij}\vec{S}_i \cdot \vec{S}_j$$

The result reveals an intra-trimmer J = -0.475(4) cm^{-1} and an inter-trimmer zJ = -0.027(2) cm^{-1} with g = 2.007(1), indicating the weak antiferromagnetic interactions both inside (Mn···Mn =

5.0 Å) and among (Mn···Mn = 9.4 Å) the $Mn(II)_3$ sub-structure, compared to the reported linear $Mn(II)_3$-based coordination polymers.[20]

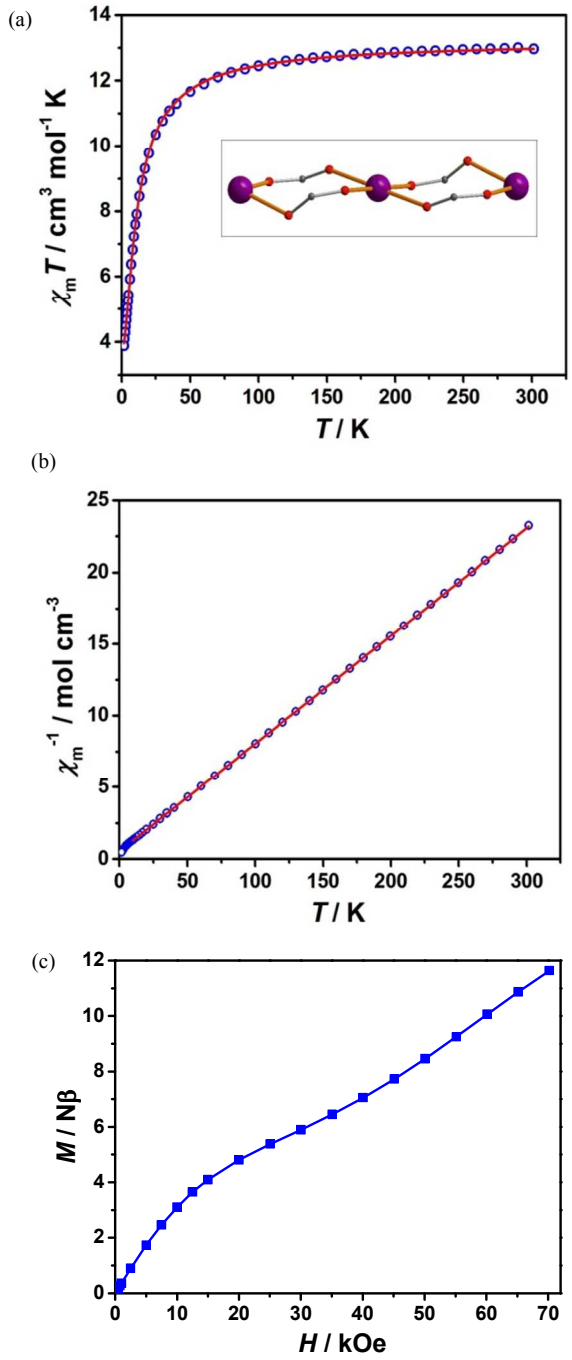

Fig. 6 (a) Temperature dependence of $\chi_M T$ in the range of 1.8-300K (the solid line is fitted to the exchange model, the insert is the scheme of the $Mn(II)_3$-subunit); (b) temperature dependence of χ_M^{-1} (The solid line is fitted to the Curie-Weiss law); and (c) the field-dependent magnetization at 2 K (the solid line is the guide to the eyes) for **1**.

On the other hand, the magnetic properties of **2** and **4** mainly come from the single ion behavior of Ni(II) and Cu(II), respectively, owing to the lack of strong magnetic interactions like **1**. At 300 K, the $\chi_M T$ values are 1.31 cm^3 mol^{-1} K for **2** (Fig. 7a) and 0.43 cm^3 mol^{-1} K for **4** (Fig. 7b). Both of them are larger than the spin-only values (1.0 for **2** and 0.375 for **4**), indicating the presence of spin-orbit coupling which is commonly observed for Ni(II) and Cu(II).[19,21] Upon cooling, the $\chi_M T$ value decrease slowly, mainly owing to the weak antiferromagnetic interaction and/or zero-field splitting. Fitting the experimental data to the Curie-Weiss law in 1.8-300 K leads to the negative Weiss constants θ = -0.83 K for **2** and -0.54 K for **4**, both of which are much smaller than that of **1**. The magnetization curves at 2 K are also in typical paramagnetic shapes as expected, reaching the saturation of 2.29 Nβ for **2** and 1.00 Nβ for **4** (Fig. 7c), respectively.

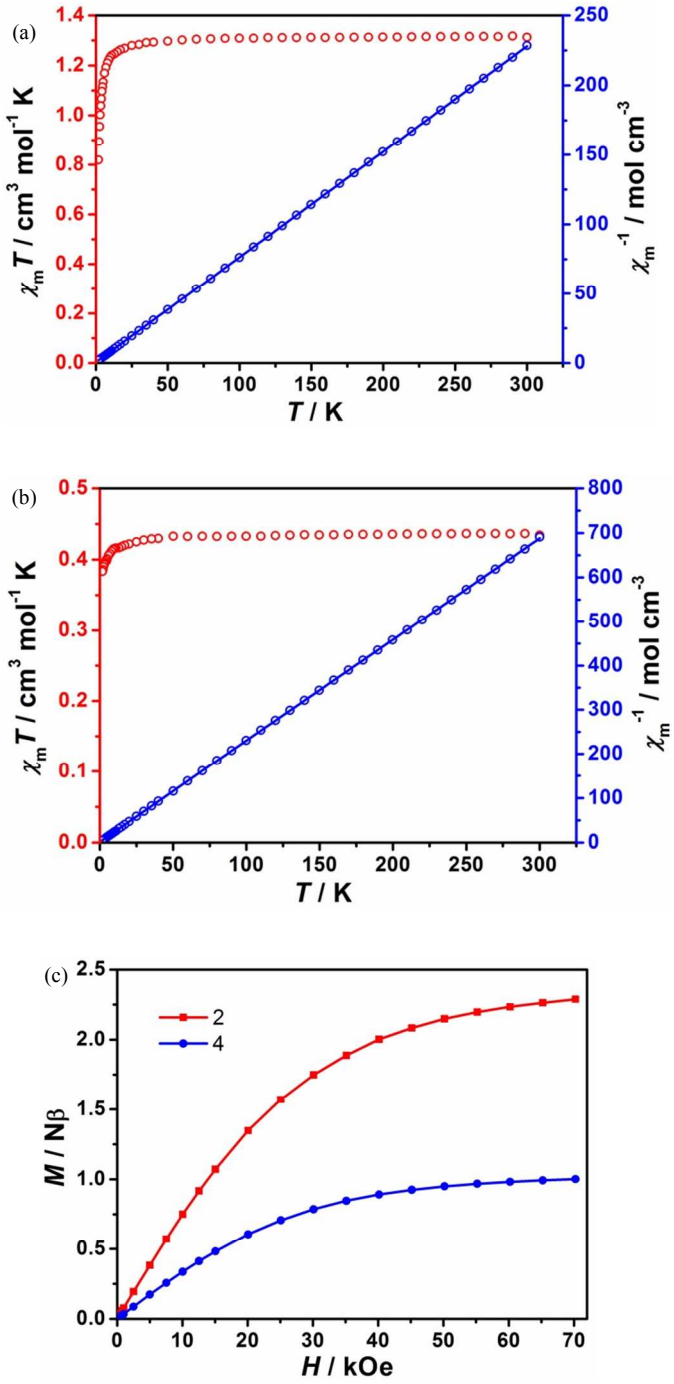

Fig. 7 (a) Temperature dependence of $\chi_M T$ (left) and χ_M^{-1} (right) in the range of 1.8-300K (the solid line is fitted to the Curie-Weiss law) for **2**, (b) Temperature dependence of $\chi_M T$ (left) and χ_M^{-1} (right) in the range of 2-300K (the solid line is fitted to the Curie-Weiss law) for **4**; and (c) The field-dependent magnetization at 2 K for **2** (red) and **4** (blue) (the solid lines are the guides to the eyes).

Luminescent property

The solid state luminescent properties of the free H_3bptc ligand and compound **3** were investigated in solid state at room temperature. The emission band with maximum observed at 484 nm upon excitation at 296 nm for H_3bptc can be attributed to the $\pi^* \rightarrow n$ or $\pi^* \rightarrow \pi$ transition (Fig. 8a).[1c,22] According to the reported literature, the free phen molecule displays strong emission around 390 nm in solid state at room temperature attributed to the $\pi^* \rightarrow \pi$ transition.[7a,23] Comparably, the emission of compound **3** observed at 453 nm (λ_{ex} = 365 nm) with a blue-shift of 31 nm (compared to free H_3bptc) and a red shift of *ca.* 40 nm (compared to free phen) can be assigned to the cooperative effect of the metal-perturbed intraligand emission of H_3bptc and phen (Fig. 8b).[24] Notably, the chelation of H_3bptc ligand to metal ions can effectively change the dihedral angle between the two phenyl rings, and reduce the loss of energy produced from radiationless decay.[24] Thus the enhancement and blue shift in compound **3** may be attributed to the altered energy level of the $\pi^* \rightarrow n$ or $\pi^* \rightarrow \pi$ transition. Different from compound **3** with d^{10} configurations, the emission bands of compound **1**, **2**, and **4** with unpaired electrons are observed around 498 nm and 520 nm with weak intensity (Fig. S4), which may be due to the ligand-field transitions (d-d) via electron or energy transfer through the partially filled d-orbitals.[25]

(a)

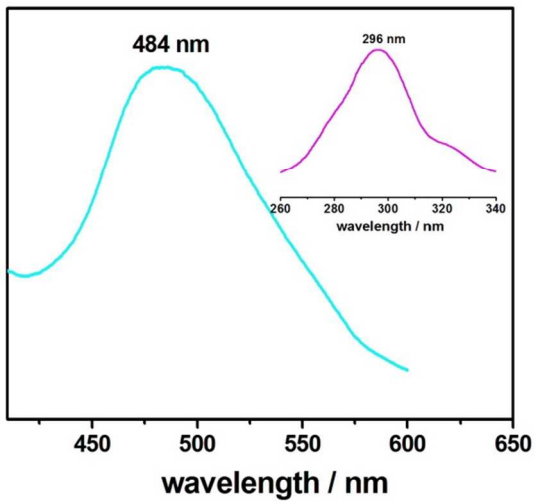

(b)

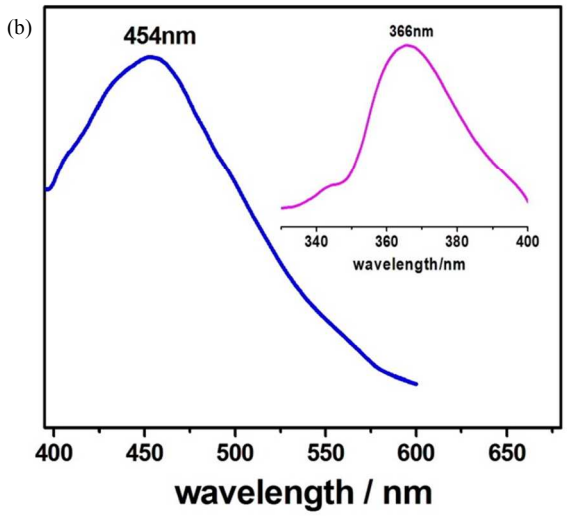

Fig. 8 (a) The excitation (insert) and emission spectra for free H_3bptc ligand and (b) compound **3** in solid state at room temperature.

Conclusions

Four new coordination polymers involving asymmetric ligand with rotatable coordination vertex and N-donor ligands have been successfully synthesized and characterized. According to single crystal X-ray analysis, compound **1** is a 3D coordination network, **2** is a 1D ladder chain-based structure, **3** and **4** are 0D dimmer-based structures. The asymmetric H_3bptc ligand has been partly or fully deprotonated and adopt different coordination modes in the compounds. Theoretical calculation on free H_3bptc shows that the thermodynamically most stable conformation is the one with dihedral angle 53.5º, while the dihedral angles are 47.3º, 56.6º, 42.2º and 35.4º in compounds **1**-**4**, respectively. The different conformations of the ligand may be due to the coordination interactions to metal ions and different coordination modes. Magnetic property studies indicate the existence of an antiferromagnetic interaction in compounds **1**, **2** and **4**. Luminescent property studies reveal that compound **3** displays intense blue emission in solid at room temperature, which may be a good candidate for a potential photoactive material.

Acknowledgements

This work was supported by the National Science Foundation of China (No. 20901018) and the Yang-cheng Scholars Foundation of Guangzhou (No. 12A002D).

Notes and references

[a] *Guangzhou Key Laboratory for Environmentally Functional Materials and Technology, School of Chemistry and Chemical Engineering, Guangzhou University, Guangzhou 510006, P. R. China. Fax: 86 02039366908; Tel: 86 02039366908; E-mail: wangjgzhu@163.com*
[b] *State Key Laboratory of Optoelectronic Materials and Technologies, School of Chemistry and Chemical Engineering, Sun Yat-Sen University, Guangzhou 510275, P. R. China*

† Electronic Supplementary Information (ESI) available: Crystallographic data in CIF format for **1**-**4**, computational details for free H_3bptc, XRPD patterns for **1**-**4**, TG curves for **1**-**4**, excitation and emission spectra for **1**, **2** and **4**, selected bond lengths and angles for **1**-**4**, hydrogen bond lengths and angles for **2** and **4**. See DOI: 10.1039/b000000x/

1 (a) H.-X. Deng, C. J. Doonan, H. Furukawa, R. B. Ferreira, J. Towne, C. B. Knobler, B. Wang and O. M. Yaghi, *Science*, 2010, **327**, 846; (b) L. E. Kreno, K. Leong, O. K. Farha, M. Allendorf, R. P. V. Duyne and J. T. Hupp, *Chem. Rev.*, 2012, **112**, 1105; (c) Y.-J Cui, Y.-F. Yue, G.-D. Qian and B.-L. Chen, *Chem. Rev.*, 2012, **112**, 1126; (d) T. Yamada, K. Otsubo, R. Makiura and H. Kitagawa, *Chem. Soc. Rev.*, 2013, **42**, 6655; (e) M. Zhao, S. Ou, and C.-D. Wu, *Acc. Chem. Res.*, 2014, **47**, 1199; (f) S.-H. Yang, X. Lin, W. Lewis, M. Suyetin, E. Bichoutskaia, J. E. Parker, C. C. Tang, D. R. Allan, P. J. Rizkallah, P. Hubberstey, N. R. Champness, K. M. Thomas, A. J. Blake and M. Schröder, *Nat. Mater.*, 2012, **11**, 710; (g) M. H. Mohamed, S. Elsaidi, L. Wojtas, T. Pham, K. A. Forrest, B. Tudor, B. Space and M. J. Zawarotko, *J. Am. Chem. Soc.*, 2012, **134**, 19556; (h) X. Bao, H. J. Shepherd, L. Salmon, G. Molnar, M.-L. Tong and A. Bousseksou, *Angew. Chem., Int. Ed.*, 2013, **52**, 1198.

2 (a) D. Yuan, D. Zhao, D. Sun and H.-C. Zhou, *Angew. Chem., Int. Ed.*, 2010, **49**, 5357; (b) Q.-K. Liu, J.-P. Ma and Y.-B. Dong, *J. Am. Chem. Soc.*, 2010, **132**, 7005; (c) Y. Yan, S. Yang, A. J. Blake, W. Lewis, E. Poirier, S. A. Barnett, N. R. Champness and M. Schröder, *Chem. Commun.*, 2011, **47**, 9995; (d) D. Sun, Z.-H. Yan, V. A. Blatov, L. Wang and D.-F. Sun, *Cryst. Growth Des.*, 2013, **13**, 1277; (e) L.-H. Cao, Y.-L. Wei, Y. Yang, H. Xu, S.-Q. Zang, H.-W. Hou and T. C. W. Mak, *Cryst. Growth Des.*, 2014, **14**, 1827; (f) L. Ma, N. Yu, S. Chen and H. Deng, *CrystEngComm*, 2013, **15**, 1352; (g) F. Guo, B. Zhu, M. Liu, X. Zhang, J. Zhang and J. Zhao, *CrystEngComm*, 2013, **15**, 6191; (h) Z. Wu, W. Sun, Y. Chai, W. Zhao, H. Wu, T. Shi and X. Yang, *CrystEngComm*, 2014, **16**, 406; (i) Z.-J. Lin and M.-L. Tong, *Coord. Chem. Rev.,* 2011, **255**, 421.

3 (a) D. Tian, Q. Chen, Y. Li, Y.-H. Zhang, Z. Chang, and X.-H. Bu, *Angew. Chem.*, 2014, **126**, 856; (b) P. V. Dau, K. K. Tanabe and S. M. Cohen, *Chem. Commun.*, 2013, **49**, 9370; (c) P. V. Dau, M. Kim and S. M. Cohen, *Chem. Sci.*, 2012, **4**, 601; (d) T. Li, J. Yang, X.-J. Hong, Y.-J. Ou, Z.-G. Gu and Y.-P Cai, *CrystEngComm*, 2014, **16**, 3848; (e) Z.-J. Lin, Y.-B. Huang, T.-F. Liu, X.-Y. Li and R. Cao, *Inorg. Chem.*, 2013, **52**, 3127; (f) S.-Q. Su, S. Wang, X.-Z. Song, S.-Y. Song, C. Qin, M. Zhu, Z.-M. Hao, S.-N. Zhao and H.-J. Zhang, *Dalton Trans.*, 2012, **41**, 4772.

4 (a) Q.-Y. Liu, Y.-L. Li, Y.-L. Wang, C.-M. Liu, L.-W. Ding and Y. Liu, *CrystEngComm*, 2014, **16**, 486; (b) S. Henke, A. Schneemann, S. Kapoor, R. Winter and R. A. Fischer, *J. Mater. Chem.*, 2012, **22**, 909; (c) D. O. Miles, D.-M. Jiang, A. D. Burrows, J. E. Halls and F. Marken, *Electrochem Commun*, 2013, **27**, 9; (d) J.-A. Hua, Y. Zhao, Q. Liu, D. Zhao, K. Chen and W.-Y. Sun, *CrystEngComm*, DOI: 10.1039/C4CE00835A.

5 (a) L. J. Murray, M. Dinca, J. Yano, S. Chavan, S. Bordiga, C. M. Brown and J. R. Long, *J. Am. Chem. Soc.*, 2010, **132**, 7856; (b) L. Luo, G.-C. Lv, P. Wang, Q. Liu, K. Chen and W.-Y. Sun, *CrystEngComm*, 2013, **15**, 9537; (c) Y.-H. Luo, F.-X. Yue, X.-Y. Yu, L.-L. Gu, H. Zhang and X. Chen, *CrystEngComm*, 2013, **15**, 8116; (d) X. Zhang, Y.-Y. Huang, Q.-P. Lin, J. Zhang and Y.-G. Yao, *Dalton Trans.*, 2013, **42**, 2294; (e) Y.-W. Li, J.-R. Li, L.-F. Wang, B.-Y. Zhou, Q. Chen and X.-H. Bu, *J. Mater. Chem. A*, 2013, **1**, 495.

6 (a) W.-J. Ji, Q.-G. Zhai, S.-N. Li, Y.-C. Jiang and M.-C. Hu, *Chem. Commun.*, 2011, **47**, 3834; (b) P. Song, B. Liu, Y.-Q. Li, J.-Z. Yang, Z.-M. Wang and X.-G. Li, *CrystEngComm*, 2012, **14**, 2296; (c) G.-H. Cui, C.-H. He, C.-H. Jiao, J.-C. Geng and V. A. Blatov, *CrystEngComm*, 2012, **14**, 4210; (d) J.-F. Liu, F.-P. Huang, H.-D. Bian and Q. Yu, *Z. Anorg. Allg. Chem.*, 2013, **639**, 2347; (e) E. Yang, Q.-R. Ding, Y. Kang, F. Wang, *Inorg. Chem. Commun.*, 2013, **36**, 195.

7 (a) J. Wang, Z.-J. Lin, Y.-C. Ou, N.-L. Yang, Y.-H. Zhang and M.-L. Tong, *Inorg. Chem.*, 2008, **47**, 190; (b) X.-Y. Wang and S. C. Sevov, *Inorg. Chem.*, 2008, **47**, 1037; (c) J. Wang, S.-H. Yang, A.-J. Zhou, Z.-Q. Liu and J. Zhao, *J. Coord. Chem.*, 2013, **66**, 2413.

8 (a) S. S.-Y. Chui, A. Siu, X. Feng, Z.-Y. Zhang, T. C. W. Mak and I. D. Williams, *Inorg. Chem. Commun.*, 2001, **4**, 467; (b) H. Kumagai, Y. Oka, M. A.-Tanaka and K. Inoue, *Inorg. Chim. Acta.*, 2002, **332**, 176; (c) A. Kyono, M. Kimata and T. Hatta, *Inorg. Chim. Acta.*, 2004, **357**, 2519; (d) E .Yang, J. Zhang, Z.-J. Li, S. Gao, Y. Kang, Y.-B. Chen, Y.-H. Wen and Y.-G. Yao, *Inorg. Chem.*, 2004, **43**, 6525; (e) S. M. Humphrey, R. A. Mole, R. I. Thompson and P. T. Wood , *Inorg. Chem.*, 2010, **49**, 3441.

9 (a) R.-Q. Zhong, R.-Q. Zou, M. Du, T. Yamada, G. Maruta, S. Takeda, J. Li and Q. Xu, *CrystEngComm*, 2010, **12**, 677; (b) S. A. Sapchenko, D. N. Dybtsev, D. G. Samsonenko and V. P. Fedin, *New J. Chem.*, 2010, **34**, 2445; (c) X.-Y. Yi, Y. Ying, H.-C. Fang, Z.-G. Gu, S.-R. Zheng, Q.-G. Zhan, L.-S. Jiang, W.-S. Li, F.-Q. Sun, Y.-P. Cai, *Inorg. Chem. Commun.*, 2011, **14**, 453; (d) G.-P. Zhou, Y.-L. Yang, R.-Q. Fan, W.-W. Cao and B. Yang, *CrystEngComm*, 2012, **14**, 193; (e) P. K. Yadav, N. Kumari, P. Pachfule, R. Banerjee and L. Mishra, *Cryst. Growth Des.*, 2012, **12**, 5311; (f) F. Guo, F. Wang, Hui Yang, X.-L. Zhang and J. Zhang, *Inorg. Chem.*, 2012, **51**, 9677.

10 (a) Z.-J. Lin, B. Xu, T.-F. Liu, M.-N. Cao, J. Lü and R. Cao, *Eur. J. Inorg. Chem.*, 2010, 3842; (b) Z.-Y. Guo, H. Xu, S.-Q. Su, J.-F. Cai, S. Dang, S.-C. Xiang, G.-D. Qian, H.-J Zhang, M. O. Keeffed and B.-L. Chen, *Chem. Commun.*, 2011, **47**, 5551; (c) Z.-J. Zhang, L.-P. Zhang, L. Wojtas, P. Nugent, M. Eddaoudi and M. J. Zaworotko, *J. Am. Chem. Soc.*, 2012, **134**, 924; (d) L.-N. Li, J.-H. Luo, S.-Y. Wang, Z.-H. Sun, T.-L. Chen and M.-C. Hong, *Cryst. Growth Des.*, 2011, **11**, 3744; (e) C.-C. Ji, J. Li, Y.-Z. Li, Z.-J. Guo and H.-G. Zheng, *CrystEngComm*, 2011, **13**, 459; (f) L.-N. Li, S.-Y. Wang, T.-L. Chen, Z.-H. Sun, J.-H. Luo and M.-C. Hong, *Cryst. Growth Des.*, 2012, **12**, 4109.

11 (a) J. Jia, M. Shao, T.-T. Jia, S.-R. Zhu, Y.-M. Zhao, F.-F. Xing and M.-X. Li, *CrystEngComm*, 2010, **12**, 1548; (b) L.-X. Sun, Y. Qi, Y.-M. Wang, Y.-X. Che and J.-M. Zheng, *CrystEngComm*, 2010, **12**, 1540; (c) J. Zhao, D.-S. Li, Z.-Z. Hu, W.-W. Dong, K. Zou, J. Y. Lu, *Inorg. Chem. Commun.*, 2011, **14**, 771; (d) Q.-P. Lin, T. Wu, S.-T. Zheng, X.-H. Bu and P.-Y. Feng, *Chem. Commun.*, 2011, **47**, 11852; (e) I. A. Ibarra, S.-H. Yang, X. Lin, A. J. Blake, P. J. Rizkallah, H. Nowell, D. R. Allan, N. R. Champness, P. Hubberstey and M. Schröder, *Chem. Commun.*, 2011, **47**, 8304; (f) X.-T. Zhang, L.-M. Fan, Z. Sun, W. Zhang, D.-C. Li, J.-M. Dou and L. Han, *Cryst. Growth Des.*, 2013, **13**, 792; (g) J. Zhao, D.-S. Li, X.-J. Ke, B. Liu, K. Zou and H.-M. Hu, *Dalton Trans.*, 2012, **41**, 2560; (h) S.-H. Yang, J.-L. Sun, A. J. Ramirez-Cuesta, S. K. Callear, W. I. F. David, D. P. Andersonl, R. Newby, A. J. Blake, J. E. Parker, C. C. Tang and M. Schröder, *Nature Chem.*, 2012, **4**, 887; (i) S.-H. Yang, A. J. Ramirez-Cuesta, M. Schröder, *Chem. Phys.*, 2014, **428**, 111.

12 (a) X.-Q. Lü, W.-X. Feng, Y.-N. Hui, T. Wei, J.-R.Song, S.-S. Zhao, W.-Y. Wong, W.-K. Wong and R. A. Jones, *Eur. J. Inorg. Chem.*, 2010, **18**, 2714; (b) M.-L. Cao, J.-J. Wu, J.-J. Liang and B.-H. Ye, *Cryst. Growth Des.*, 2010, **10**, 4934; (c) G.-F. Zi, F.-R. Zhang, L. Xiang, Y. Chen, W.-H. Fang and H.-B. Song, *Dalton Trans.*, 2010, **39**, 4048; (d) H.-L. Wang, D.-P. Zhang, D.-F. Sun, Y.-T Chen, K. Wang, Z.-H. Ni, L.-J. Tian and J.-Z. Jiang, *CrystEngComm*, 2010, **12**, 1096; (e) N. Domracheva, A. Pyataev, R. Manapov, M. Gruzdev, U. Chervonova and A. Kolker, *Eur. J. Inorg. Chem.*, 2011, 1291; (f) S.-Q. Su, W. Chen, C. Qin, S.-Y. Song, Z.-Y. Guo, G.-H. Li, X.-Z Song, M. Zhu, S. Wang, Z.-M. Hao and H.-J. Zhang, *Cryst. Growth Des.*, 2012, **12**, 1808; (g) H.-L. Hsiao, C.-J. Wu, W. Hsu, C.-W. Yeh, M.-Y. Xie, W.-J. Huang and J.-D. Chen, *CrystEngComm*, 2012, **14**, 8143.

13 B. Liu, B. Liu, L.-Y. Pang, G.-P. Yang, L. Cui, Y.-Y. Wang and Q.-Z. Shi, *CrystEngComm*, 2013, **15**, 5205.

14 (a) J. Wang, Y.-H. Zhang and M.-L. Tong. *Chem. Commun.*, 2006, 3166 ; (b) J. Wang, S. Hu and M.-L. Tong. *Eur. J. Inorg. Chem.*, 2006, 2069; (c) J. Wang, Z.-J. Lin, Y.-C. Ou, Y. Shen, R. Herchel and M.-L. Tong. *Chem. Eur. J.*, 2008, **24**, 7218 ; (d) J. Wang, Y.-C. Ou, Y. Shen, L. Yun, J.-D. Leng, Z.-J. Lin and M.-L. Tong, *Cryst. Growth Des.,* 2009, **9**, 2442.

15 (a) A. D. Becke, *J. Chem. Phys.*, 1993, **98**, 1372; (b) C. Lee, W. Yang and R. G. Parr, *Phys. Rev. B*, 1988, **37**, 785.

16 (a) W. J. Hehre, R. Ditchfield and J. A. Pople, *J. Chem. Phys.*, 1972, **56**, 2257; (b) M. J. Frisch, J. A. Pople and J. S. Binkley, *J. Chem. Phys.*, 1984, **80**, 3265.

17 M. J. Frisch, *et al*. Gaussian 09, Revision B.01, Inc., Wallingford, CT, 2009.

18 G. M. Sheldrick, *SHELXTL97*, program for cystal structure refinement, University of Göttingen, Germany, 1997.

19 O. Kahn, *Molecular Magnetism*; VCH Publisher: New York, 1993.

20 (a) C.-B. Ma, M.-Q. Hu, H. Chen, M. Wang, C.-X. Zhang, C.-N. Chen and Q.-T. Liu, *CrystEngComm*, 2010, **12**, 1467; (b) L.-F. Ma, M.-L. Han, J.-H. Qin, L.-Y. Wang and M. Du, *Inorg. Chem.*, 2012, **51**, 9431; (c) W.-X. Chen, G.-L. Zhang, L.-S. Long, R.-B. Huang and L.-S. Zheng, *Dalton Trans.*, 2011, **40**, 10237.

21 (a) C. M. Nagaraja, R. Haldar, T. K. Maji and C. N. R. Rao, *Cryst. Growth Des.*, 2012, **12**, 975; (b) C. N′u˜nez, R. Bastida, A. Mac′ıas, L. Valencia, N. I. Neuman, A. C. Rizzi, C. D. Brondino, P. J. Gonz′alez, J. L. Capelo and C. Lodeiro, *Dalton Trans.*, 2010, **39**, 11654; (c) D. Žilić, B. Rakvin, D. Milić, D. Pajić, I. Đilović, M. Cametti and Z. Džolić, *Dalton Trans.*, 2014, **43**, 11877.

22 (a) Z.-J. Lin, B. Xu, T.-F. Liu, M.-N. Cao, J. Lu and R. Cao, *Eur. J. Inorg. Chem.*, 2010, 3842; (b) K. Liu, Y. Peng, F. Yang, D.-X. Ma, G.-H. Li, Z. Shi and S.-H. Feng, *CrystEngComm*, 2014, **16**, 4382.

23 (a) S.-Q. Zhang, F.-L. Jiang, M.-Y. Wu, L. Chen, J.-H. Luo and M.-C. Hong, *CrystEngComm*, 2013, **15**, 3992; (b) X. Shi, G.-S. Zhu, Q.-R. Fang, G. Wu, G. Tian, R.-W. Wang, D.-L. Zhang, M. Xue, S.-L. Qiu, *Eur. J. Inorg. Chem.*, 2004, 185.

24 (a) F.-L. Liu, L.-L. Zhang, R.-M. Wang, J. Sun, Z. Chen, X.-P, Wang and D.-F. Sun, *CrystEngComm*, 2014, **16**, 2917; (b) J.-Z. Gu, A. M. Kirillov, J. Wu, D.-Y. Lv, Y. Tang, and J.-C. Wu, *CrystEngComm*, 2013, **15**, 10287; (c) Y. Zhang, B.-B. Guo, L. Li, S.-F. Liu and G. Li, *Cryst. Growth Des.,* 2013, **13**, 377.

25 (a) J. R. Lakowicz, *Principle of Fluorescence Spectroscop*y, Springer, New York, 2006, 3rd edn; (b) M. D. Allendorf, C. A. Bauer, R. K. Bhaktaa and R. J. T. Houka, *Chem. Soc. Rev.*, 2009, **38**, 1330; (c) J. Zhao, X.-L. Wang, X. Shi, Q.-H. Yang and C. Li, *Inorg. Chem.* , 2011, **50**, 3198; (d) M. Yang, Z.-J. Ouyang, W.-B. Chen, R.-F. Zhou, N. Li and W. Dong, *CrystEngComm*, 2013, **15**, 8529.

Structures and properties of coordination polymers involving asymmetric biphenyl-3,2′,5′-tricarboxylate

Jie Zhao,[a] Li-Qiong Xie,[a] Ying-Ming Ma,[a] Ai-Ju Zhou,[a] Wen Dong,[a] Jing Wang*[a], Yan-Cong Chen[b] and Ming-Liang Tong[b]

Conformations' stability and coordination modes of an asymmetric polycarboxylate ligand (H_3bptc) and properties of its compounds have been investigated.